

## Probing Gluon Spin-Momentum Correlations in Transversely Polarized Protons through Midrapidity Isolated Direct Photons in $p^\uparrow + p$ Collisions at $\sqrt{s} = 200$ GeV

U. A. Acharya,<sup>20</sup> C. Aidala,<sup>40</sup> Y. Akiba,<sup>53,54,†</sup> M. Alfred,<sup>22</sup> V. Andrieux,<sup>40</sup> N. Apadula,<sup>27</sup> H. Asano,<sup>33,53</sup> B. Azmoun,<sup>7</sup> V. Babintsev,<sup>23</sup> N. S. Bandara,<sup>39</sup> K. N. Barish,<sup>8</sup> S. Bathe,<sup>5,54</sup> A. Bazilevsky,<sup>7</sup> M. Beaumier,<sup>8</sup> R. Belmont,<sup>11,46</sup> A. Berdnikov,<sup>56</sup> Y. Berdnikov,<sup>56</sup> L. Bichon,<sup>64</sup> B. Blankenship,<sup>64</sup> D. S. Blau,<sup>32,43</sup> J. S. Bok,<sup>45</sup> M. L. Brooks,<sup>35</sup> J. Bryslawski,<sup>5,8</sup> V. Bumazhnov,<sup>23</sup> S. Campbell,<sup>12</sup> V. Canoa Roman,<sup>59</sup> R. Cervantes,<sup>59</sup> C. Y. Chi,<sup>12</sup> M. Chiu,<sup>7</sup> I. J. Choi,<sup>24</sup> J. B. Choi,<sup>29,\*</sup> Z. Citron,<sup>65</sup> M. Connors,<sup>20,54</sup> R. Corliss,<sup>59</sup> Y. Corrales Morales,<sup>35</sup> N. Cronin,<sup>59</sup> M. Csanád,<sup>15</sup> T. Csörgő,<sup>16,66</sup> T. W. Danley,<sup>47</sup> M. S. Daugherty,<sup>1</sup> G. David,<sup>7,59</sup> K. DeBlasio,<sup>44</sup> K. Dehmelt,<sup>59</sup> A. Denisov,<sup>23</sup> A. Deshpande,<sup>54,59</sup> E. J. Desmond,<sup>7</sup> A. Dion,<sup>59</sup> D. Dixit,<sup>59</sup> J. H. Do,<sup>67</sup> A. Drees,<sup>59</sup> K. A. Drees,<sup>6</sup> J. M. Durham,<sup>35</sup> A. Durum,<sup>23</sup> A. Enokizono,<sup>53,55</sup> H. En'yo,<sup>53</sup> R. Esha,<sup>59</sup> S. Esumi,<sup>63</sup> B. Fadem,<sup>41</sup> W. Fan,<sup>59</sup> N. Feege,<sup>59</sup> D. E. Fields,<sup>44</sup> M. Finger,<sup>9</sup> M. Finger, Jr.,<sup>9</sup> D. Fitzgerald,<sup>40</sup> S. L. Fokin,<sup>32</sup> J. E. Frantz,<sup>47</sup> A. Franz,<sup>7</sup> A. D. Frawley,<sup>19</sup> Y. Fukuda,<sup>63</sup> C. Gal,<sup>59</sup> P. Gallus,<sup>13</sup> P. Garg,<sup>3,59</sup> H. Ge,<sup>59</sup> M. Giles,<sup>59</sup> F. Giordano,<sup>24</sup> Y. Goto,<sup>53,54</sup> N. Grau,<sup>2</sup> S. V. Greene,<sup>64</sup> M. Grosse Perdekamp,<sup>24</sup> T. Gunji,<sup>10</sup> H. Guragain,<sup>20</sup> T. Hachiya,<sup>42,53,54</sup> J. S. Haggerty,<sup>7</sup> K. I. Hahn,<sup>17</sup> H. Hamagaki,<sup>10</sup> H. F. Hamilton,<sup>1</sup> S. Y. Han,<sup>17,31</sup> J. Hanks,<sup>59</sup> M. Harvey,<sup>61</sup> S. Hasegawa,<sup>28</sup> T. O. S. Haseler,<sup>20</sup> X. He,<sup>20</sup> T. K. Hemmick,<sup>59</sup> J. C. Hill,<sup>27</sup> K. Hill,<sup>11</sup> A. Hodges,<sup>20</sup> R. S. Hollis,<sup>8</sup> K. Homma,<sup>21</sup> B. Hong,<sup>31</sup> T. Hoshino,<sup>21</sup> N. Hotvedt,<sup>27</sup> J. Huang,<sup>7</sup> S. Huang,<sup>64</sup> K. Imai,<sup>28</sup> M. Inaba,<sup>63</sup> A. Iordanova,<sup>8</sup> D. Isenhower,<sup>1</sup> D. Ivanishchev,<sup>51</sup> B. V. Jacak,<sup>59</sup> M. Jezghani,<sup>20</sup> Z. Ji,<sup>59</sup> X. Jiang,<sup>35</sup> B. M. Johnson,<sup>7,20</sup> D. Jouan,<sup>49</sup> D. S. Jumper,<sup>24</sup> J. H. Kang,<sup>67</sup> D. Kapukchyan,<sup>8</sup> S. Karthas,<sup>59</sup> D. Kawall,<sup>39</sup> A. V. Kazantsev,<sup>32</sup> V. Khachatryan,<sup>59</sup> A. Khazadzev,<sup>51</sup> A. Khatiwada,<sup>35</sup> C. Kim,<sup>8,31</sup> E.-J. Kim,<sup>29</sup> M. Kim,<sup>57</sup> D. Kincses,<sup>15</sup> A. Kingan,<sup>59</sup> E. Kistenev,<sup>7</sup> J. Klatsky,<sup>19</sup> P. Kline,<sup>59</sup> T. Koblesky,<sup>11</sup> D. Kotov,<sup>51,56</sup> S. Kudo,<sup>63</sup> B. Kuryis,<sup>15</sup> K. Kurita,<sup>55</sup> Y. Kwon,<sup>67</sup> J. G. Lajoie,<sup>27</sup> D. Larionova,<sup>56</sup> A. Lebedev,<sup>27</sup> S. Lee,<sup>67</sup> S. H. Lee,<sup>27,40,59</sup> M. J. Leitch,<sup>35</sup> Y. H. Leung,<sup>59</sup> N. A. Lewis,<sup>40</sup> X. Li,<sup>35</sup> S. H. Lim,<sup>35,52,67</sup> M. X. Liu,<sup>35</sup> V.-R. Loggins,<sup>24</sup> S. Lökös,<sup>15</sup> D. A. Loomis,<sup>40</sup> K. Lovasz,<sup>14</sup> D. Lynch,<sup>7</sup> T. Majoros,<sup>14</sup> Y. I. Makdisi,<sup>6</sup> M. Makek,<sup>68</sup> V. I. Manko,<sup>32</sup> E. Mannel,<sup>7</sup> M. McCumber,<sup>35</sup> P. L. McGaughey,<sup>35</sup> D. McGlinchey,<sup>11,35</sup> C. McKinney,<sup>24</sup> M. Mendoza,<sup>8</sup> A. C. Mignerey,<sup>38</sup> A. Milov,<sup>65</sup> D. K. Mishra,<sup>4</sup> J. T. Mitchell,<sup>7</sup> Iu. Mitrakov,<sup>56</sup> M. Mitrakova,<sup>56</sup> G. Mitsuka,<sup>30,54</sup> S. Miyasaka,<sup>53,62</sup> S. Mizuno,<sup>53,63</sup> M. M. Mondal,<sup>59</sup> P. Montuenga,<sup>24</sup> T. Moon,<sup>31,67</sup> D. P. Morrison,<sup>7</sup> B. Mulilo,<sup>31,53</sup> T. Murakami,<sup>33,53</sup> J. Murata,<sup>53,55</sup> K. Nagai,<sup>62</sup> K. Nagashima,<sup>21</sup> T. Nagashima,<sup>55</sup> J. L. Nagle,<sup>11</sup> M. I. Nagy,<sup>15</sup> I. Nakagawa,<sup>53,54</sup> K. Nakano,<sup>53,62</sup> C. Nattrass,<sup>60</sup> S. Nelson,<sup>18</sup> T. Niida,<sup>63</sup> R. Nouicer,<sup>7,54</sup> T. Novák,<sup>16,66</sup> N. Novitzky,<sup>59,63</sup> G. Nukazuka,<sup>53,54</sup> A. S. Nyanin,<sup>32</sup> E. O'Brien,<sup>7</sup> C. A. Ogilvie,<sup>27</sup> J. D. Orjuela Koop,<sup>11</sup> J. D. Osborn,<sup>40,48</sup> A. Oskarsson,<sup>36</sup> G. J. Ottino,<sup>44</sup> K. Ozawa,<sup>30,63</sup> V. Pantuev,<sup>25</sup> V. Papavassiliou,<sup>45</sup> J. S. Park,<sup>57</sup> S. Park,<sup>53,57,59</sup> S. F. Pate,<sup>45</sup> M. Patel,<sup>27</sup> W. Peng,<sup>64</sup> D. V. Perepelitsa,<sup>7,11</sup> G. D. N. Perera,<sup>45</sup> D. Yu. Peressouko,<sup>32</sup> C. E. PerezLara,<sup>59</sup> J. Perry,<sup>27</sup> R. Petti,<sup>7</sup> M. Phipps,<sup>7,24</sup> C. Pinkenburg,<sup>7</sup> R. P. Pisani,<sup>7</sup> M. Potekhin,<sup>7</sup> A. Pun,<sup>47</sup> M. L. Purschke,<sup>7</sup> P. V. Radzevich,<sup>56</sup> N. Ramasubramanian,<sup>59</sup> K. F. Read,<sup>48,60</sup> D. Reynolds,<sup>58</sup> V. Riabov,<sup>43,51</sup> Y. Riabov,<sup>51,56</sup> D. Richford,<sup>5</sup> T. Rinn,<sup>24,27</sup> S. D. Rolnick,<sup>8</sup> M. Rosati,<sup>27</sup> Z. Rowan,<sup>5</sup> J. Runchey,<sup>27</sup> A. S. Safonov,<sup>56</sup> T. Sakaguchi,<sup>7</sup> H. Sako,<sup>28</sup> V. Samsonov,<sup>43,51</sup> M. Sarsour,<sup>20</sup> S. Sato,<sup>28</sup> B. Schaefer,<sup>64</sup> B. K. Schmoll,<sup>60</sup> K. Sedgwick,<sup>8</sup> R. Seidl,<sup>53,54</sup> A. Sen,<sup>27,60</sup> R. Seto,<sup>8</sup> A. Sexton,<sup>38</sup> D. Sharma,<sup>59</sup> D. Sharma,<sup>59</sup> I. Shein,<sup>23</sup> T.-A. Shibata,<sup>53,62</sup> K. Shigaki,<sup>21</sup> M. Shimomura,<sup>27,42</sup> T. Shioya,<sup>63</sup> P. Shukla,<sup>4</sup> A. Sickles,<sup>24</sup> C. L. Silva,<sup>35</sup> D. Silvermyr,<sup>36</sup> B. K. Singh,<sup>3</sup> C. P. Singh,<sup>3</sup> V. Singh,<sup>3</sup> M. Slunečka,<sup>9</sup> K. L. Smith,<sup>19</sup> M. Snowball,<sup>35</sup> R. A. Soltz,<sup>34</sup> W. E. Sondheim,<sup>35</sup> S. P. Sorensen,<sup>60</sup> I. V. Sourikova,<sup>7</sup> P. W. Stankus,<sup>48</sup> S. P. Stoll,<sup>7</sup> T. Sugitate,<sup>21</sup> A. Sukhanov,<sup>7</sup> T. Sumita,<sup>53</sup> J. Sun,<sup>59</sup> Z. Sun,<sup>14</sup> J. Sziklai,<sup>66</sup> K. Tanida,<sup>28,54,57</sup> M. J. Tannenbaum,<sup>7</sup> S. Tarafdar,<sup>64,65</sup> A. Taranenko,<sup>43</sup> G. Tarnai,<sup>14</sup> R. Tieulent,<sup>20,37</sup> A. Timilsina,<sup>27</sup> T. Todoroki,<sup>53,54,63</sup> M. Tomášek,<sup>13</sup> C. L. Towell,<sup>1</sup> R. S. Towell,<sup>1</sup> I. Tserruya,<sup>65</sup> Y. Ueda,<sup>21</sup> B. Ujvari,<sup>14</sup> H. W. van Hecke,<sup>35</sup> J. Velkovska,<sup>64</sup> M. Virius,<sup>13</sup> V. Vrba,<sup>13,26</sup> N. Vukman,<sup>68</sup> X. R. Wang,<sup>45,54</sup> Y. S. Watanabe,<sup>10</sup> C. P. Wong,<sup>20,35</sup> C. L. Woody,<sup>7</sup> C. Xu,<sup>45</sup> Q. Xu,<sup>64</sup> L. Xue,<sup>20</sup> S. Yalcin,<sup>59</sup> Y. L. Yamaguchi,<sup>59</sup> H. Yamamoto,<sup>63</sup> A. Yanovich,<sup>23</sup> J. H. Yoo,<sup>31</sup> I. Yoon,<sup>57</sup> H. Yu,<sup>45,50</sup> I. E. Yushmanov,<sup>32</sup> W. A. Zajc,<sup>12</sup> A. Zelenski,<sup>6</sup> S. Zharko,<sup>56</sup> and L. Zou<sup>8</sup>

(PHENIX Collaboration)

<sup>1</sup>Abilene Christian University, Abilene, Texas 79699, USA<sup>2</sup>Department of Physics, Augustana University, Sioux Falls, South Dakota 57197, USA<sup>3</sup>Department of Physics, Banaras Hindu University, Varanasi 221005, India<sup>4</sup>Bhabha Atomic Research Centre, Bombay 400 085, India<sup>5</sup>Baruch College, City University of New York, New York, New York 10010, USA

- <sup>6</sup>Collider-Accelerator Department, Brookhaven National Laboratory, Upton, New York 11973-5000, USA
- <sup>7</sup>Physics Department, Brookhaven National Laboratory, Upton, New York 11973-5000, USA
- <sup>8</sup>University of California-Riverside, Riverside, California 92521, USA
- <sup>9</sup>Charles University, Ovocný trh 5, Praha 1, 116 36 Prague, Czech Republic
- <sup>10</sup>Center for Nuclear Study, Graduate School of Science, University of Tokyo, 7-3-1 Hongo, Bunkyo, Tokyo 113-0033, Japan
- <sup>11</sup>University of Colorado, Boulder, Colorado 80309, USA
- <sup>12</sup>Columbia University, New York, New York 10027 and Nevis Laboratories, Irvington, New York 10533, USA
- <sup>13</sup>Czech Technical University, Zikova 4, 166 36 Prague 6, Czech Republic
- <sup>14</sup>Debrecen University, H-4010 Debrecen, Egyetem tér 1, Hungary
- <sup>15</sup>ELTE, Eötvös Loránd University, H-1117 Budapest, Pázmány P. s. 1/A, Hungary
- <sup>16</sup>Eszterházy Károly University, Károly Róbert Campus, H-3200 Gyöngyös, Mátrai út 36, Hungary
- <sup>17</sup>Ewha Womans University, Seoul 120-750, Korea
- <sup>18</sup>Florida A&M University, Tallahassee, Florida 32307, USA
- <sup>19</sup>Florida State University, Tallahassee, Florida 32306, USA
- <sup>20</sup>Georgia State University, Atlanta, Georgia 30303, USA
- <sup>21</sup>Hiroshima University, Kagamiyama, Higashi-Hiroshima 739-8526, Japan
- <sup>22</sup>Department of Physics and Astronomy, Howard University, Washington, D.C. 20059, USA
- <sup>23</sup>IHEP Protvino, State Research Center of Russian Federation, Institute for High Energy Physics, Protvino 142281, Russia
- <sup>24</sup>University of Illinois at Urbana-Champaign, Urbana, Illinois 61801, USA
- <sup>25</sup>Institute for Nuclear Research of the Russian Academy of Sciences, prospekt 60-letiya Oktyabrya 7a, Moscow 117312, Russia
- <sup>26</sup>Institute of Physics, Academy of Sciences of the Czech Republic, Na Slovance 2, 182 21 Prague 8, Czech Republic
- <sup>27</sup>Iowa State University, Ames, Iowa 50011, USA
- <sup>28</sup>Advanced Science Research Center, Japan Atomic Energy Agency, 2-4 Shirakata Shirane, Tokai-mura, Naka-gun, Ibaraki-ken 319-1195, Japan
- <sup>29</sup>Jeonbuk National University, Jeonju 54896, Korea
- <sup>30</sup>KEK, High Energy Accelerator Research Organization, Tsukuba, Ibaraki 305-0801, Japan
- <sup>31</sup>Korea University, Seoul 02841, Korea
- <sup>32</sup>National Research Center “Kurchatov Institute,” Moscow, 123098 Russia
- <sup>33</sup>Kyoto University, Kyoto 606-8502, Japan
- <sup>34</sup>Lawrence Livermore National Laboratory, Livermore, California 94550, USA
- <sup>35</sup>Los Alamos National Laboratory, Los Alamos, New Mexico 87545, USA
- <sup>36</sup>Department of Physics, Lund University, Box 118, SE-221 00 Lund, Sweden
- <sup>37</sup>IPNL, CNRS/IN2P3, Univ Lyon, Universit Lyon 1, F-69622 Villeurbanne, France
- <sup>38</sup>University of Maryland, College Park, Maryland 20742, USA
- <sup>39</sup>Department of Physics, University of Massachusetts, Amherst, Massachusetts 01003-9337, USA
- <sup>40</sup>Department of Physics, University of Michigan, Ann Arbor, Michigan 48109-1040, USA
- <sup>41</sup>Muhlenberg College, Allentown, Pennsylvania 18104-5586, USA
- <sup>42</sup>Nara Women’s University, Kita-uoya Nishi-machi Nara 630-8506, Japan
- <sup>43</sup>National Research Nuclear University, MEPhI, Moscow Engineering Physics Institute, Moscow 115409, Russia
- <sup>44</sup>University of New Mexico, Albuquerque, New Mexico 87131, USA
- <sup>45</sup>New Mexico State University, Las Cruces, New Mexico 88003, USA
- <sup>46</sup>Physics and Astronomy Department, University of North Carolina at Greensboro, Greensboro, North Carolina 27412, USA
- <sup>47</sup>Department of Physics and Astronomy, Ohio University, Athens, Ohio 45701, USA
- <sup>48</sup>Oak Ridge National Laboratory, Oak Ridge, Tennessee 37831, USA
- <sup>49</sup>IPN-Orsay, Univ. Paris-Sud, CNRS/IN2P3, Université Paris-Saclay, BPI, F-91406 Orsay, France
- <sup>50</sup>Peking University, Beijing 100871, People’s Republic of China
- <sup>51</sup>PNPI, Petersburg Nuclear Physics Institute, Gatchina, Leningrad region 188300, Russia
- <sup>52</sup>Pusan National University, Pusan 46241, Korea
- <sup>53</sup>RIKEN Nishina Center for Accelerator-Based Science, Wako, Saitama 351-0198, Japan
- <sup>54</sup>RIKEN BNL Research Center, Brookhaven National Laboratory, Upton, New York 11973-5000, USA
- <sup>55</sup>Physics Department, Rikkyo University, 3-34-1 Nishi-Ikebukuro, Toshima, Tokyo 171-8501, Japan
- <sup>56</sup>Saint Petersburg State Polytechnic University, St. Petersburg 195251, Russia
- <sup>57</sup>Department of Physics and Astronomy, Seoul National University, Seoul 151-742, Korea
- <sup>58</sup>Chemistry Department, Stony Brook University, SUNY, Stony Brook, New York 11794-3400, USA
- <sup>59</sup>Department of Physics and Astronomy, Stony Brook University, SUNY, Stony Brook, New York 11794-3800, USA
- <sup>60</sup>University of Tennessee, Knoxville, Tennessee 37996, USA
- <sup>61</sup>Texas Southern University, Houston, Texas 77004, USA
- <sup>62</sup>Department of Physics, Tokyo Institute of Technology, Oh-okayama, Meguro, Tokyo 152-8551, Japan
- <sup>63</sup>Tomonaga Center for the History of the Universe, University of Tsukuba, Tsukuba, Ibaraki 305, Japan
- <sup>64</sup>Vanderbilt University, Nashville, Tennessee 37235, USA

<sup>65</sup>Weizmann Institute, Rehovot 76100, Israel<sup>66</sup>Institute for Particle and Nuclear Physics, Wigner Research Centre for Physics, Hungarian Academy of Sciences (Wigner RCP, RMKI) H-1525 Budapest 114, P.O. Box 49, Budapest, Hungary<sup>67</sup>Yonsei University, IPAP, Seoul 120-749, Korea<sup>68</sup>Department of Physics, Faculty of Science, University of Zagreb, Bijenička c. 32 HR-10002 Zagreb, Croatia

(Received 1 March 2021; revised 26 July 2021; accepted 10 August 2021; published 12 October 2021)

Studying spin-momentum correlations in hadronic collisions offers a glimpse into a three-dimensional picture of proton structure. The transverse single-spin asymmetry for midrapidity isolated direct photons in  $p^\uparrow + p$  collisions at  $\sqrt{s} = 200$  GeV is measured with the PHENIX detector at the Relativistic Heavy Ion Collider (RHIC). Because direct photons in particular are produced from the hard scattering and do not interact via the strong force, this measurement is a clean probe of initial-state spin-momentum correlations inside the proton and is in particular sensitive to gluon interference effects within the proton. This is the first time direct photons have been used as a probe of spin-momentum correlations at RHIC. The uncertainties on the results are a 50-fold improvement with respect to those of the one prior measurement for the same observable, from the Fermilab E704 experiment. These results constrain gluon spin-momentum correlations in transversely polarized protons.

DOI: 10.1103/PhysRevLett.127.162001

Unlike lepton-hadron scattering, proton-proton collisions are sensitive to gluon scattering at leading order. Direct photons are produced *directly* in the hard scattering of partons and, because they do not interact via the strong force, are a phenomenologically clean probe of the structure of the proton. At large transverse momentum, direct photons are produced at leading order via the quantum chromodynamics (QCD) 2-to-2 hard scattering subprocesses quark-gluon Compton scattering ( $g + q \rightarrow \gamma + q$ ) and quark-antiquark annihilation ( $\bar{q} + q \rightarrow \gamma + g$ ). Compton scattering dominates at midrapidity [1] because the proton is being probed at moderate longitudinal momentum fraction  $x$  where gluons are the primary constituents of the proton. Thus midrapidity direct photon measurements are a clean probe of gluon structure within the proton.

Transverse single-spin asymmetries (TSSAs) in hadronic collisions are sensitive to various spin-momentum correlations, i.e., correlations between the directions of the spin and momentum of partons and/or hadrons involved in a scattering event. In collisions between one transversely polarized proton and one unpolarized proton, the TSSA describes the azimuthal-angular dependence of particle production relative to the transverse polarization direction. TSSAs have been measured to be as large as 40% in forward charged pion production [2–5] and significantly nonzero forward neutral pion asymmetries have been measured with transverse momentum up to  $p_T \approx 7$  GeV/ $c$  [6]. In this context,  $p_T$  serves as a proxy for a hard-scattering energy ( $Q$ ) that is well

into the perturbative regime of QCD. Next-to-leading-order perturbative QCD calculations which only include effects from high energy parton scattering predict that these asymmetries should be small and fall off as  $m_q/Q$  [7], where  $m_q$  is the bare mass of the quark. Thus, to explain these large TSSAs, they must be considered in the context of the dynamics present in proton-proton collisions that cannot be calculated perturbatively, namely, dynamics describing proton structure and/or the process of hadronization.

One approach toward explaining the large measured TSSAs is through transverse-momentum-dependent (TMD) functions. These functions depend on the soft-scale-parton transverse momentum,  $k_T$ , in addition to the partonic longitudinal momentum fraction  $x$  and  $Q$ , where  $k_T \ll Q$ . TMD functions can be directly extracted from measurements that are sensitive to two momentum scales, such as semi-inclusive deep-inelastic scattering (SIDIS) where the angle and energy of the scattered electron can be used to directly measure the hard-scale  $Q$  and the transverse momentum of the measured hadron relates to the soft scales  $k_T$  of TMD parton distribution functions (PDFs) and fragmentation functions. The Sivers function is a PDF that describes the structure of the transversely polarized proton and correlates the transverse spin of the proton and  $k_T$  of the parton within it [8]. The quark Sivers function has been extracted through polarized SIDIS measurements, but the gluon Sivers function has remained comparatively less constrained because SIDIS is not sensitive to gluons at leading order [9]. The direct photon TSSA in proton-proton collisions has been shown to be sensitive to the gluon Sivers function [10], but the  $k_T$  moment of TMD functions must be used to apply these functions to the single-scale inclusive TSSAs measured in proton-proton collisions.

Twist-3 correlation functions are another approach toward describing TSSAs. Unlike TMD functions,

Published by the American Physical Society under the terms of the Creative Commons Attribution 4.0 International license. Further distribution of this work must maintain attribution to the author(s) and the published article's title, journal citation, and DOI. Funded by SCOAP<sup>3</sup>.

collinear twist-3 correlation functions depend only on a single scale, the hard scale  $Q$ . Twist-3 functions describe spin-momentum correlations generated by the quantum mechanical interference between scattering off of one parton versus scattering off of two. There are two different types: the quark-gluon-quark ( $qqg$ ) correlation functions and the trigluon ( $ggg$ ) correlation function. In the context of proton structure,  $qqg$  correlation functions describe the interference between scattering off of a single quark in the proton versus scattering off of a quark which carries the same flavor and the same momentum fraction and an additional gluon. Analogously, the trigluon correlation describes the interference between scattering off of one gluon in the proton versus scattering off of two. Additional twist-3 collinear correlation functions describing spin-momentum correlations in the process of hadronization also exist, but are not relevant to the production of direct photons. Collinear twist-3 functions have been shown to be related to the  $k_T$  moment of TMD functions [11,12]. For example, the Efremov-Teryaev-Qiu-Sterman (ETQS) function is a  $qqg$  correlation function for the polarized proton [13–15] that is related to the  $k_T$  moment of the Sivers TMD PDF. The ETQS function has also been extracted from fits to inclusive TSSAs in proton-proton collisions [16,17], and the forward direct photon TSSA has been suggested to be dominated by this ETQS function [18]. The fact that both TMD and collinear twist-3 functions are nonzero reflects that scattering partons do in fact interact with the color fields present inside the proton, which goes beyond traditional assumptions present in hadronic collision studies.

Multiple observables can provide sensitivity to the  $ggg$  correlation function. Midrapidity inclusive hadron TSSA measurements are sensitive to gluon spin-momentum correlations in the proton but also include potential effects from hadronization and final-state color interactions. Heavy flavor production at the Relativistic Heavy Ion Collider (RHIC) is dominated by gluon-gluon fusion and thus particularly sensitive to gluons in the proton. A heavy flavor hadron TSSA measurement [19] has been used to estimate the trigluon correlation function in the transversely polarized proton assuming no effects from hadronization or final-state color interactions [20]. The midrapidity isolated direct photon TSSA is instead a clean probe of the trigluon correlation function because it is insensitive to hadronization effects as well as final-state color interactions [21].

The only previously published direct photon TSSA measurement is the Fermilab E704 result, which used a 200 GeV/ $c$  polarized proton beam on an unpolarized proton target ( $\sqrt{s} = 19.4$  GeV). It was found to be consistent with zero to within 20% for  $2.5 < p_T^\gamma < 3.1$  GeV/ $c$  [22]. The PHENIX results presented in this Letter measure photons with  $p_T^\gamma > 5$  GeV/ $c$  with total uncertainties up to a factor of 50 smaller than the E704 measurements. This measurement will constrain trigluon correlations in transversely polarized protons.

The presented direct photon measurement was performed with the PHENIX experiment in the central rapidity region  $|\eta| < 0.35$ , using  $p^\uparrow + p$  collisions at  $\sqrt{s} = 200$  GeV. The dataset was collected in 2015 and corresponds to an integrated luminosity of approximately  $60 \text{ pb}^{-1}$ . Direct photons were reconstructed using similar techniques to a previously published direct photon cross section result at  $\sqrt{s} = 200$  GeV [23]. The asymmetry was measured with transversely polarized proton beams at RHIC where the clockwise and counterclockwise beams had an average polarization of  $0.58 \pm 0.02$  and  $0.60 \pm 0.02$ , respectively [24]. Collisions between bunches are spaced 106 ns apart and the polarization direction changes bunch-to-bunch such that two statistically independent asymmetries can be measured with the same particle yields through sorting them by the polarization direction in one beam, effectively averaging over the polarization in the other beam. These two independent measurements serve as a cross check and are averaged together to calculate the final asymmetry.

The PHENIX central detector comprises two nearly back-to-back arms each covering  $\Delta\phi = \pi/2$  in azimuth and  $|\eta| < 0.35$  in pseudorapidity. Photons are identified through clusters in the electromagnetic calorimeter (EMCal), which has two detector arms: the west and the east. The west arm comprises four sectors of sampling lead-scintillator (PbSc) calorimeters with granularity  $\delta\phi \times \delta\eta = 0.011 \times 0.011$  and the east arm comprises two more PbSc sectors along with two sectors of Čerenkov lead-glass (PbGl) calorimeters with granularity  $\delta\phi \times \delta\eta = 0.008 \times 0.008$  [25].

The PHENIX central tracking system uses pad chambers and a drift chamber to measure the position of charged particle tracks [26]. The beam-beam counters (BBC) are far-forward arrays of quartz Čerenkov radiators that cover the full azimuth and  $3.0 < |\eta| < 3.9$  [27]. They measure the position of the vertex in the beam direction, for which a 30 cm vertex cut around the nominal collision point is applied. The minimum-bias trigger fires on crossings where at least one charged particle is measured in each arm of the BBC. Events with high- $p_T$  photons are selected through an EMCal-based high-energy photon trigger that is taken in coincidence with this minimum-bias trigger.

All photons used in the asymmetry calculation are required to pass the following cuts. A shower shape cut selects clusters whose energy distribution is consistent with a parametrized profile from a photon shower. This reduces the contribution of clusters from hadrons along with merged photons from high energy  $\pi^0$  decays, which resolve as a single cluster in the EMCal. A time-of-flight cut suppresses the contribution of EMCal noise, where the timing of the cluster is measured by the EMCal and the time zero reference of the event is provided by the BBC. A charged-track-veto cut eliminates clusters that geometrically match with a charged track and uses the track position measured directly in front of the EMCal. This cut reduces the background from electrons as well as charged hadrons that were not eliminated by the shower shape cut.

Direct photon candidates are also required to pass tagging cuts that reduce the hadronic decay background by eliminating photons that are tagged as coming from either  $\pi^0 \rightarrow \gamma\gamma$  or  $\eta \rightarrow \gamma\gamma$  decays. The candidate direct photon is matched with a partner photon in the same event and same EMCal arm, which has passed a minimum-energy cut of 0.5 GeV. A photon is considered tagged as coming from a  $\pi^0 \rightarrow \gamma\gamma$  ( $\eta \rightarrow \gamma\gamma$ ) decay if it is matched into a photon pair with invariant mass  $105 < M_{\gamma\gamma} < 165$  MeV/ $c^2$  ( $480 < M_{\gamma\gamma} < 620$  MeV/ $c^2$ ), which corresponds roughly to a  $\pm 2\sigma$  window around the observed  $\pi^0$  and  $\eta$  peaks.

Additionally, direct photon candidates have to pass an isolation cut, which further reduces the contribution of decay photons [23]. Reference [1] estimates that the contribution of the next-to-leading-order fragmentation photons to the isolated direct photon sample is less than 15% for photons with  $p_T > 5$  GeV/ $c$ . The photon isolation cut requires that the sum of the particles' energy surrounding the photon in a cone of radius  $r = \sqrt{(\Delta\eta)^2 + (\Delta\phi)^2} < 0.4$  radians be less than 10% of the candidate photon's energy:  $E_{\text{cone}} < E_\gamma \cdot 10\%$ . To be included in the cone sum energy,  $E_{\text{cone}}$ , an EMCal cluster must have energy larger than 0.15 GeV and a charged track needs to have a momentum above 0.2 GeV/ $c$ . To provide a more inclusive sample of the particles surrounding the photon, the clusters and tracks that are included in the  $E_{\text{cone}}$  sum are only required to pass a minimum set of quality cuts. The charged track veto cut is still used to ensure charged particles are not double counted by the energy that they deposit in the EMCal. The shower-shape cut is not applied to EMCal clusters to ensure that neutral hadrons and charged hadrons that were not reconstructed as charged tracks can still contribute to  $E_{\text{cone}}$ .

The asymmetry measurement is formed from photons that satisfy these criteria, using similar techniques to previously published PHENIX TSSAs which include Refs. [19] and [28]. The TSSA is determined using the relative luminosity formula:

$$A_N = \frac{1}{P \langle \cos(\phi) \rangle} \frac{N^\uparrow - \mathcal{R}N^\downarrow}{N^\uparrow + \mathcal{R}N^\downarrow}, \quad (1)$$

where  $\mathcal{R} = \mathcal{L}^\uparrow/\mathcal{L}^\downarrow$  is the relative luminosity of collisions for when the beam was polarized up versus down.  $P$  is the average polarization of the beam, and  $\langle \cos(\phi) \rangle$  is the acceptance factor accounting for the azimuthal coverage of each detector arm. In Eq. (1),  $N$  refers to the particle yield and the up ( $\uparrow$ ) or down ( $\downarrow$ ) arrow superscripts refer to the direction of the beam polarization. The asymmetries are calculated separately for each arm of the detector and averaged together for the final result, weighted by the statistical uncertainty.

The main source of direct-photon background comes from decay photons that were not eliminated by the tagging cut because their partner photon was not measured. This can occur because the partner photon was out of acceptance, hit a dead area of the detector, or did not pass the minimum-energy cut. To calculate the isolated direct-photon asymmetry,  $A_N^{\text{dir}}$ , the candidate isolated direct-photon asymmetry,  $A_N^{\text{iso}}$ , must be corrected for the contribution from background:

$$A_N^{\text{dir}} = \frac{A_N^{\text{iso}} - r_{\pi^0} A_N^{\text{iso},\pi^0} - r_\eta A_N^{\text{iso},\eta}}{1 - r_{\pi^0} - r_\eta}. \quad (2)$$

This expression removes the effects of background asymmetries from isolated  $\pi^0$  photons,  $A_N^{\text{iso},\pi^0}$ , and isolated  $\eta$  photons,  $A_N^{\text{iso},\eta}$ , where  $r_{\pi^0}$  and  $r_\eta$  are the background fractions due to photons from  $\pi^0$  and  $\eta$  decays, respectively. Because the midrapidity  $\pi^0$  and  $\eta$  TSSAs have been measured to be consistent with zero to high statistical precision [28] and their isolated asymmetries were also confirmed to be consistent with zero,  $A_N^{\text{iso},\pi^0}$  and  $A_N^{\text{iso},\eta}$  are set to zero in Eq. (2). The systematic uncertainty due to setting the background asymmetries to zero dominates the total systematic uncertainty of the direct-photon asymmetry for all  $p_T$  bins. It is assigned by integrating the inclusive midrapidity  $\pi^0$  and  $\eta$  TSSAs over photon  $p_T$  and propagating their uncertainties through Eq. (2).

The background fraction calculation is performed by taking the ratio of measured photon yields:  $N_{\text{tag}}^{\text{iso},h}/N^{\text{iso}}$ , where  $N^{\text{iso}}$  is the isolated direct photon candidate sample.  $N_{\text{tag}}^{\text{iso},h}$  is the number of photons that were tagged as coming from a diphoton decay of hadron  $h$  and pass the photon pair isolation cut,  $E_{\text{cone}} - E_{\text{partner}} < E_\gamma \cdot 10\%$ , which subtracts off the energy of the partner photon,  $E_{\text{partner}}$ . Tagged photons that pass this cut would have been included in the isolated direct photon candidate sample had their partner photon not been detected. Simulations are used to calculate how to convert from the number of tagged decay photons to the number of decay photons where the partner photon was missed. The background fraction  $r_h$ , for photons from  $\pi^0$  and  $\eta$  meson decays, is calculated separately to account for their differences in particle production and decay kinematics,

$$r_h = R_h \frac{N_{\text{tag}}^{\text{iso},h}}{N^{\text{iso}}}, \quad (3)$$

where  $R_h$  is the one-miss ratio for the decay of hadron  $h$ . It is the ratio in single particle Monte Carlo of the number of photons for which only one of the simulated decay photons was reconstructed to the number of photons in which both decay photons were reconstructed [23]. These simulations include the geometry, resolution, and configuration of the

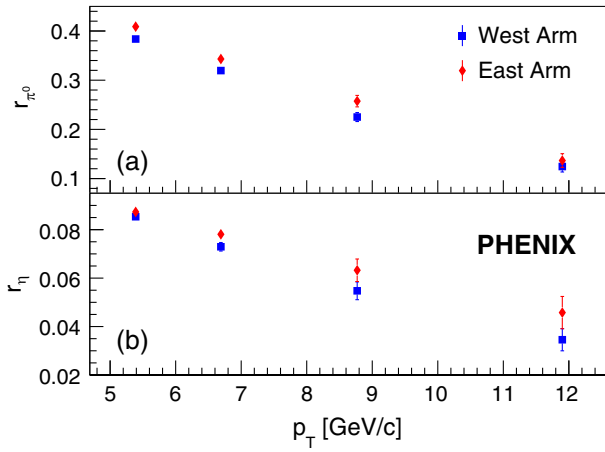


FIG. 1. The fractional contribution of photons from (a)  $\pi^0$  and (b)  $\eta$  decays to the isolated direct photon candidate sample.

dead areas of the EMCAL and use the previously measured  $\pi^0$  [29] and  $\eta$  [30] cross sections. The background fractions for photons from  $\pi^0$  ( $\eta$ ) decays are plotted in Fig. 1 and are systematically larger in the east arm versus the west due to the PbGl sectors having slightly more dead area compared to the PbSc sectors. The contribution of decay photons from sources heavier than  $\eta$  mesons is estimated to be less than 3% with respect to the measured background and so an even smaller percentage of the total direct photon sample. The uncertainty on the background fraction is propagated through Eq. (2) to assign an additional systematic uncertainty to the direct-photon asymmetry.

A similar method to Eq. (3) is used to find the contribution of merged  $\pi^0$  decay photons. The equivalent  $R_h$  is calculated using simulated  $h \rightarrow \gamma\gamma$  decays, taking the ratio of the number of reconstructed EMCAL clusters produced by merged decay photons divided by the number of reconstructed clusters associated with a single decay photon. The contribution from merged photon clusters was found to be less than 0.2%, small compared to the up to 50% background fraction due to the one-miss effects, and the contribution from merged  $\eta$  decays was confirmed to be negligible.

An additional systematic study is performed by calculating the asymmetry with the square root formula:

$$A_N = \frac{1}{P\langle\cos(\phi)\rangle} \frac{\sqrt{N_L^\uparrow N_R^\downarrow} - \sqrt{N_L^\downarrow N_R^\uparrow}}{\sqrt{N_L^\uparrow N_R^\downarrow} + \sqrt{N_L^\downarrow N_R^\uparrow}}, \quad (4)$$

where the  $L$  and  $R$  subscripts refer to yields to the left and to the right of the polarized-beam-going direction, respectively. This result is verified to be consistent with the relative luminosity formula results from Eq. (1) and the differences between these results are assigned as an additional systematic uncertainty due to possible variations in detector performance and beam conditions. The systematic

TABLE I. The measured  $A_N$  of isolated direct photons in  $p^\uparrow + p$  collisions at  $\sqrt{s} = 200$  GeV as a function of  $p_T$ . An additional scale uncertainty of 3.4% due to the polarization uncertainty is not included.

$\langle p_T \rangle$ [GeV/c]	$A_N^{\text{dir}}$	$\sigma_{\text{stat}}$	$\sigma_{\text{syst}}$
5.39	-0.00 049 2	0.00 299	0.00 341
6.69	0.00 247	0.00 404	0.00 252
8.77	0.00 777	0.00 814	0.00 159
11.88	0.00 278	0.0105	0.00 106

uncertainty due to setting the background asymmetries to zero dominates the total systematic uncertainty by an order of magnitude for all  $p_T$  bins except for the highest  $p_T$  bin, where it is only slightly larger than the difference between the square root formula and relative luminosity formula. Another study using bunch shuffling found no additional systematic effects. Bunch shuffling is a technique that randomizes the bunch-by-bunch beam polarization directions to confirm that the variations present in the data are consistent with what is expected by statistical variation.

The results for the  $A_N$  of isolated direct photons,  $A_N^{\text{dir}}$ , at midrapidity in  $p^\uparrow + p$  collisions at  $\sqrt{s} = 200$  GeV are shown in Table I and in Fig. 2, where the shaded (gray) bands represent the systematic uncertainty and the vertical bars represent the statistical uncertainty. The measurement is consistent with zero to within 1% across the entire  $p_T$  range. Figure 2 also shows predictions from collinear twist-3 correlation functions. The solid (green) curve shows the contribution of  $qgq$  correlation functions to the direct-photon asymmetry which is calculated using functions that were published in Ref. [18] that are integrated over the  $|\eta| < 0.35$  pseudorapidity range of the PHENIX central arms. This calculation includes contributions from the  $qgq$  correlation functions present in both the polarized and unpolarized proton, including the ETQS function

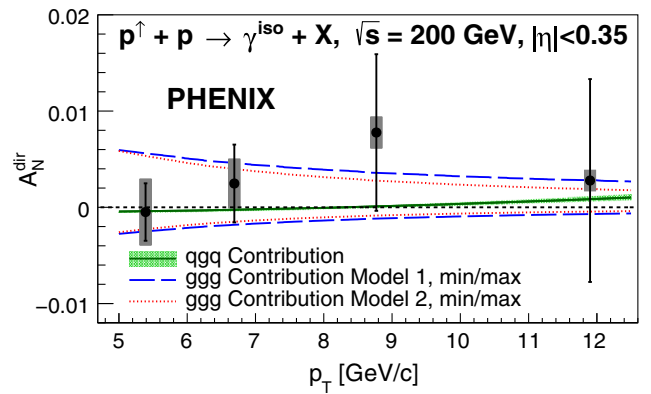


FIG. 2. Transverse single-spin asymmetry of isolated direct photons measured at midrapidity  $|\eta| < 0.35$  in  $p^\uparrow + p$  collisions at  $\sqrt{s} = 200$  GeV. An additional scale uncertainty of 3.4% due to the polarization uncertainty is not shown.

which is extracted from a global fit in Ref. [17]. The error band plotted with the solid (green) curve in Fig. 2 includes uncertainties propagated from fits to data, but does not include uncertainties associated with assuming functional forms. Quark-flavor dependence is not considered in these calculations, including  $qgq$  correlators. Direct-photon production in  $p + p$  collisions is four times more sensitive to the up quark than the down quark in the proton because of the factor of electric charge squared in the production cross section.

Given the small predicted contributions from  $qgq$  correlation functions to the midrapidity direct photon TSSA, this measurement can provide a clean extraction of the  $ggg$  function. The predicted ranges for the trigluon correlation function's contribution to the direct-photon asymmetry are also plotted in Fig. 2. The dashed (blue) and dotted (red) curves use results that were published in Ref. [20] and were reevaluated as a function of photon  $p_T$  for pseudorapidity  $\eta = 0$  [31]. Models 1 and 2 assume different functional forms for the trigluon correlation function in terms of the collinear leading-twist gluon PDF; no uncertainties are available for these curves. As shown in Fig. 2, this measurement has the statistical precision, especially at low  $p_T$ , to constrain the trigluon correlation function.

In summary, the TSSA of midrapidity isolated direct photons was measured by the PHENIX experiment to be consistent with zero in the presented  $p_T$  range, with uncertainties as low as 0.4% in the lowest  $p_T$  bins. This is the first time direct photons have been used to probe transversely polarized proton collisions at RHIC and the first measurement of this TSSA in almost 30 years, with significantly higher  $p_T$  reach and up to a 50-fold improvement in uncertainty. Direct photons are a clean probe of proton structure with no contributions from final-state QCD effects and at midrapidity are particularly sensitive to gluon dynamics. When included in the global analysis of world TSSA data, this measurement will constrain gluon spin-momentum correlations in the transversely polarized proton for  $x \approx x_T = 0.05\text{--}0.18$ , marking an important step toward creating a more three-dimensional picture of proton structure.

We thank the staff of the Collider-Accelerator and Physics Departments at Brookhaven National Laboratory and the staff of the other PHENIX participating institutions for their vital contributions. We also thank D. Pitonyak and S. Yoshida for helpful discussions. We acknowledge support from the Office of Nuclear Physics in the Office of Science of the Department of Energy, the National Science Foundation, Abilene Christian University Research Council, Research Foundation of SUNY, and Dean of the College of Arts and Sciences, Vanderbilt University (USA), Ministry of Education, Culture, Sports, Science, and Technology and the Japan Society for the Promotion of Science (Japan), Natural Science Foundation of China (People's Republic of China), Croatian Science Foundation and Ministry of Science and Education

(Croatia), Ministry of Education, Youth and Sports (Czech Republic), Centre National de la Recherche Scientifique, Commissariat à l'Énergie Atomique, and Institut National de Physique Nucléaire et de Physique des Particules (France), Bundesministerium für Bildung und Forschung, Deutscher Akademischer Austausch Dienst, and Alexander von Humboldt Stiftung (Germany), J. Bolyai Research Scholarship, EFOP, the New National Excellence Program (ÚNKP), NKFIH, and OTKA (Hungary), Department of Atomic Energy and Department of Science and Technology (India), Israel Science Foundation (Israel), Basic Science Research and SRC (CENuM) Programs through NRF funded by the Ministry of Education and the Ministry of Science and ICT (Korea), Physics Department, Lahore University of Management Sciences (Pakistan), Ministry of Education and Science, Russian Academy of Sciences, Federal Agency of Atomic Energy (Russia), VR and Wallenberg Foundation (Sweden), the U.S. Civilian Research and Development Foundation for the Independent States of the Former Soviet Union, the Hungarian American Enterprise Scholarship Fund, the US-Hungarian Fulbright Foundation, and the US-Israel Binational Science Foundation.

\*Deceased.

†PHENIX Spokesperson.  
akiba@rcf.rhic.bnl.gov

- [1] A. Adare *et al.* (PHENIX Collaboration), High  $p_T$  direct photon and  $\pi^0$  triggered azimuthal jet correlations and measurement of  $k_T$  for isolated direct photons in  $p + p$  collisions at  $\sqrt{s} = 200$  GeV, *Phys. Rev. D* **82**, 072001 (2010).
- [2] R. D. Klem, J. E. Bowers, H. W. Courant, H. Kagan, M. L. Marshak, E. A. Peterson, K. Ruddick, W. H. Dragoset, and J. B. Roberts, Measurement of Asymmetries of Inclusive Pion Production in Proton Proton Interactions at 6-GeV/ $c$  and 11.8-GeV/ $c$ , *Phys. Rev. Lett.* **36**, 929 (1976).
- [3] D. L. Adams *et al.* (FNAL-E704 Collaboration), Analyzing power in inclusive  $\pi^+$  and  $\pi^-$  production at high  $x_F$  with a 200-GeV polarized proton beam, *Phys. Lett. B* **264**, 462 (1991).
- [4] C. E. Allgower *et al.*, Measurement of analyzing powers of  $\pi^+$  and  $\pi^-$  produced on a hydrogen and a carbon target with a 22-GeV/ $c$  incident polarized proton beam, *Phys. Rev. D* **65**, 092008 (2002).
- [5] I. Arsene *et al.* (BRAHMS Collaboration), Single Transverse Spin Asymmetries of Identified Charged Hadrons in Polarized  $p + p$  Collisions at  $\sqrt{s} = 62.4$  GeV, *Phys. Rev. Lett.* **101**, 042001 (2008).
- [6] J. Adam *et al.* (STAR Collaboration), Comparison of transverse single-spin asymmetries for forward  $\pi^0$  production in polarized  $pp$ ,  $pAl$  and  $pAu$  collisions at nucleon pair c.m. energy  $\sqrt{s_{NN}} = 200$  GeV, *Phys. Rev. D* **103**, 072005 (2021).
- [7] G. L. Kane, J. Pumplin, and W. Repko, Transverse Quark Polarization in Large  $p_T$  Reactions,  $e^+e^-$  Jets, and Lep-toproduction: A Test of QCD, *Phys. Rev. Lett.* **41**, 1689 (1978).

- [8] D. W. Sivers, Single spin production asymmetries from the hard scattering of point-like constituents, *Phys. Rev. D* **41**, 83 (1990).
- [9] C. Adolph *et al.* (COMPASS Collaboration), First measurement of the Sivers asymmetry for gluons using SIDIS data, *Phys. Lett. B* **772**, 854 (2017).
- [10] R. M. Godbole, A. Kaushik, A. Misra, and S. Padval, Probing the gluon sivers function through direct photon production at RHIC, *Phys. Rev. D* **99**, 014003 (2019).
- [11] D. Boer, P. J. Mulders, and F. Pijlman, Universality of  $T$  odd effects in single spin and azimuthal asymmetries, *Nucl. Phys.* **B667**, 201 (2003).
- [12] X. Ji, J.-W. Qiu, W. Vogelsang, and F. Yuan, A Unified Picture for Single Transverse-Spin Asymmetries in Hard Processes, *Phys. Rev. Lett.* **97**, 082002 (2006).
- [13] A. V. Efremov and O. V. Teryaev, QCD asymmetry and polarized Hadron structure functions, *Phys. Lett.* **150B**, 383 (1985).
- [14] J. Qiu and G. F. Sterman, Single transverse spin asymmetries in direct photon production, *Nucl. Phys.* **B378**, 52 (1992).
- [15] J. Qiu and G. F. Sterman, Single transverse spin asymmetries in hadronic pion production, *Phys. Rev. D* **59**, 014004 (1998).
- [16] K. Kanazawa, Y. Koike, A. Metz, and D. Pitonyak, Towards an explanation of transverse single-spin asymmetries in proton-proton collisions: The role of fragmentation in collinear factorization, *Phys. Rev. D* **89**, 111501(R) (2014).
- [17] J. Cammarota, L. Gamberg, Z.-B. Kang, J. A. Miller, D. Pitonyak, A. Prokudin, T. C. Rogers, and N. Sato (Jefferson Lab Angular Momentum Collaboration), Origin of single transverse-spin asymmetries in high-energy collisions, *Phys. Rev. D* **102**, 054002 (2020).
- [18] K. Kanazawa, Y. Koike, A. Metz, and D. Pitonyak, Transverse single-spin asymmetries in  $p^\uparrow p \rightarrow \gamma X$  from quark-gluon-quark correlations in the proton, *Phys. Rev. D* **91**, 014013 (2015).
- [19] C. Aidala *et al.* (PHENIX Collaboration), Cross section and transverse single-spin asymmetry of muons from open heavy-flavor decays in polarized  $p + p$  collisions at  $\sqrt{s} = 200$  GeV, *Phys. Rev. D* **95**, 112001 (2017).
- [20] Y. Koike and S. Yoshida, Probing the three-gluon correlation functions by the single spin asymmetry in  $p^\uparrow p \rightarrow DX$ , *Phys. Rev. D* **84**, 014026 (2011).
- [21] Y. Koike and S. Yoshida, Three-gluon contribution to the single spin asymmetry in Drell-Yan and direct-photon processes, *Phys. Rev. D* **85**, 034030 (2012).
- [22] D. L. Adams *et al.* (E704 Collaboration), Measurement of single spin asymmetry for direct photon production in p p collisions at 200-GeV/c, *Phys. Lett. B* **345**, 569 (1995).
- [23] A. Adare *et al.* (PHENIX Collaboration), Direct-photon production in  $p + p$  collisions at  $\sqrt{s} = 200$  GeV at mid-rapidity, *Phys. Rev. D* **86**, 072008 (2012).
- [24] W. D. Schmidke *et al.* (The RHIC Polarimetry Group Collaboration), RHIC polarization for Runs 917, <https://technotes.bnl.gov/Home/ViewTechNote/209057> (2018).
- [25] L. Aphecetche *et al.* (PHENIX Collaboration), PHENIX calorimeter, *Nucl. Instrum. Methods Phys. Res., Sect. A* **499**, 521 (2003).
- [26] K. Adcox *et al.* (PHENIX Collaboration), PHENIX central arm tracking detectors, *Nucl. Instrum. Methods Phys. Res., Sect. A* **499**, 489 (2003).
- [27] M. Allen *et al.*, PHENIX inner detectors, *Nucl. Instrum. Methods Phys. Res., Sect. A* **499**, 549 (2003).
- [28] U. A. Acharya *et al.* (PHENIX Collaboration), Transverse single-spin asymmetries of midrapidity  $\pi^0$  and  $\eta$  mesons in polarized  $p + p$  collisions at  $\sqrt{s} = 200$  GeV, *Phys. Rev. D* **103**, 052009 (2021).
- [29] A. Adare *et al.* (PHENIX Collaboration), Inclusive cross-section and double helicity asymmetry for  $\pi^0$  production in  $p + p$  collisions at  $\sqrt{s} = 200$  GeV: Implications for the polarized gluon distribution in the proton, *Phys. Rev. D* **76**, 051106 (2007).
- [30] A. Adare *et al.* (PHENIX Collaboration), Cross section and double helicity asymmetry for  $\eta$  mesons and their comparison to neutral pion production in p + p collisions at  $\sqrt{s} = 200$  GeV, *Phys. Rev. D* **83**, 032001 (2011).
- [31] The trigluon Model 1 and Model 2 curves in Fig. 2 were provided by S. Yoshida, while D. Pitonyak provided the quark-gluon-quark curve.